

The lithium-rich giant stars puzzle: New observational trends for a general-mass-loss scenario

R. de la Reza¹

Observatorio Nacional (ON), MCT, Rua José Cristino 77, Sao Cristovao, Rio de Janeiro -Brazil
e-mail: ramirodelareza@yahoo.com

ABSTRACT

The existence of one percent of lithium-rich giant stars among normal, lithium-poor giant stars continues to be poorly explained. By merging two catalogues - one containing 10,535 lithium-rich giant stars with lithium abundances ranging from 1.5 to 4.9 dex, and the other detecting infrared sources - we have found 421 clump giant stars and 196 first-ascending giant stars with infrared excesses indicating stellar mass losses. The clump stars are the most lithium-rich. Approximately 5.8 percent of these stars appear to episodically lose mass in periods of approximately 10^4 years or less, while the remaining stars ceased their mass loss and maintained their lithium for nearly 10^7 years. We propose a scenario in which all giant stars with masses below two solar masses undergo prompt lithium enrichment with mass-ejection episodes. We suggest that the mass loss results from internal angular-momentum transport. It is possible that a transitory instability, perhaps of magnetic origin, rapidly transports the nuclear material responsible for the lithium enrichment to the stellar surface and triggers shell ejections. Additionally, the strong mass loss in some lithium-rich stars during their evolution activates their chromospheres, as observed in ultraviolet spectra. Furthermore, intense episodic mass losses in these stages led to the observable formation of complex organic and inorganic particles, as detected in near-infrared spectra. In contrast to first-ascending giant stars, helium flashes during the clump can contribute to additional lithium enrichment alongside the aforementioned process. The combination of these two lithium sources may explain the much higher observed lithium abundances in clump stars, as well as their observed infrared excesses. If our scenario –based on a universal and rapid lithium enrichment episode process– is correct, it could explain the rarity of lithium-rich giant stars.

Key words. stars: evolution–stars: interiors–stars: mass loss–stars: chemically peculiar– stars: late type

1. Introduction

Since the first Li-rich K giant star was serendipitously discovered by Wallerstein & Sneden (1982), with a lithium abundance of 2.95 dex, a complete explanation of this phenomenon has not appeared up to now. This situation is commonly referred to in the literature as part of the 'lithium giant stars puzzle'. In fact, if the standard model of stellar evolution can predict lithium abundance values below 1.5 dex, larger values than this require non-standard physical scenarios. After 1982, several Li-rich stars were discovered, primarily by larger surveys such as the LAMOST survey (Gao et al. 2019, hereafter GA19), the GALAH survey (Martell et al. 2021, hereafter MA21), the GAIA-ESO survey (Smiljanic et al. 2018), and Casey et al. (2016), among others. Even though several thousands of Li-rich red giant stars have been detected today, they still represent only 1–1.5% of the Li-poor red giant low-mass stars with masses between ~ 0.8 and $\sim 2 M_{\odot}$. The absence of an explanation for this permanent fraction of $\sim 1\%$ can be considered as the other part of the puzzle. Regarding the proposed scenarios to try to solve this Li giant stars problem, a dedicated paper on the collection of them has been presented by Yan & Shi (2022). As a general view, these scenarios are divided into a stellar internal origin of the Li enrichment and an external one, or a mixture of them. The internal ones use the known Cameron-Fowler mechanism (Cameron & Fowler 1971), based mainly on the process in which the produced ${}^7\text{Li}$ is transported to the surface convective stellar envelope, where it can be observed. The external mechanisms require an external source of Li as planets or sub-stellar objects, which

are ingested by the external stellar red-giant convective zone (Siess & Livio 1999; Carlberg et al. 2012; Aguilera-Gómez et al. 2016; Stephan et al. 2020; Soares-Furtado et al. 2021; Aguilera-Gómez et al. 2022, 2023; Tayar et al. 2023; Behmard et al. 2023). However, these external mechanisms require, as a validity test, not only that the planetary or sub-stellar source of Li appears as an excess in the star, but also the presence of other elements such as Be and B. Nevertheless, Castilho et al. (1999) and Melo et al. (2005) did not detect any observed excess of Be in Li-rich giant stars. The same is also the case for the boron element, which is the hardest to destroy in internal stellar layers, making it the most severe test for the engulfing scenario.

The boron feature in the UV *Hubble* spectra at 1200 Å does not show the presence of any excess of boron in some very Li-rich and Li-rich giant stars (Drake et al. 2018). It must also be noted that the engulfing mechanism cannot explain the existence of what are called the very Li-rich giant stars with Li abundances larger than 2.2 dex (Aguilera-Gómez et al. 2016). Concerning the mixture cases, Casey et al. (2019) proposed that a tidal spin-up effect produced by a binary companion (see also Costa et al. 2002) can induce sufficiently fast mixing in the giant stellar interior, which is capable of driving ${}^7\text{Li}$ production. This prediction of the presence of binary stars is especially invoked for the red-clump (RC) giant stage of evolution. However, a recent work by Castro-Tapia et al. (2024), investigating the radial velocities of quite a large sample of 1400 giants, does not find evidence of a binary nature of Li-rich giant stars, at least for RC giant stars (see also Tayar et al. 2023). Apart from these examples, there are other more specific cases of Li production, such as a merging be-

tween a red giant star and a He white dwarf (Holanda et al. 2020; Zhang et al. 2020). The study of Li-rich and very Li-rich giant stars, which means up to Li abundances of ~ 5 dex, requires an approach that goes further than the standard and non-standard models known in the literature. Concerning a standard study in which the stellar convective motions are the only mixture mechanism, a recent, different approach was taken by Li et al. (2024) showing that in the absence of a Li-depleting mechanism, and progenitor stars with Li abundances that exceed 3.3 dex, the majority of stars will be Li-rich. However, in this approach the Li problem brings a new problem, which is the need to search for an unknown and very efficient extra Li-depletion process that affects the largest and major part of the giant stars, which are in fact Li-poor. Concerning non-standard models, such as those based on thermohaline instability and rotation-induced mixing processes (Charbonnel & Lagarde 2010), these are not able, at least for first-ascending giant (i.e. RGB) stars, to produce larger increases in Li abundances. As a result of this work, where we investigated the internal Li-enrichment process in low-mass giant stars, we propose that the entire Li-enrichment scenario is a consequence of the evolution of a single star. This approach has no limitations regarding the observed Li abundances between 1.5 and ~ 5.0 dex.

This paper is structured in the following way. Section 2 is devoted to all aspects referring to the IR (infrared) excesses found here for Li-rich giant stars. In Sect. 3, a general scenario with the problems involving the angular momentum and the corresponding nuclear reactions are presented. Section 4 is dedicated to the general Li properties in giant stars. Finally, a discussion and conclusion are presented in Sect. 5.

2. Measurements of the infrared excesses

To our knowledge, few works have been dedicated to the measurements of IR excesses for a larger number of giant stars such as MA21, Mallick et al. (2022), and Sneden et al. (2022), among others. For our research here, we are guided by the work of MA21 because it provides more details of their search for IR excesses. MA21 considered, as they call it, 'clean' WISE detections, which are sources that do not show image confusion. This is done following the instruction in the WISE manual, with the WISE `cc_flags` confusion flag set to 0000, corresponding to the four W1 ($3.4\mu\text{m}$), W2 ($4.6\mu\text{m}$), W3 ($12\mu\text{m}$), and W4 ($22\mu\text{m}$) magnitude colours. Additionally, a second condition was used in which the `ph_qual` photometric quality flag is set to A for W1 and W4.

From a set of 1862 giant stars, mainly from the GALAH catalogue, with clean WISE detections, they detected only three (two RC stars and one RGB star) with larger excesses W1–W4 larger than 0.5 (see their Figure 9). We believe, as we show later, that this very low number is the result of the extremely strict detection conditions used by these authors, considering only the mentioned A quality flag. Therefore, we decided to explore the whole LAMOST catalogue containing 10,525 Li-rich giant stars (GA19) under less strict WISE detection conditions. For this purpose, we retained the first confusion flag, keeping sources with the 0000 confusion condition, but gradually relaxed the `ph_flag`, exploring conditions other than A (which represents the signal-to-noise ratio $S/N > 10$) to levels B ($S/N < 10$) and finally to level C ($S/N < 3$). We eliminated, a priori, all IR sources presenting upper-limit values in W1 and W4. The main condition is that all of our accepted W1 and W4 values fulfil the measure of W1–W4 of being larger than or equal to 0.5 in order to be considered as good indicators of the infrared excesses. The detailed

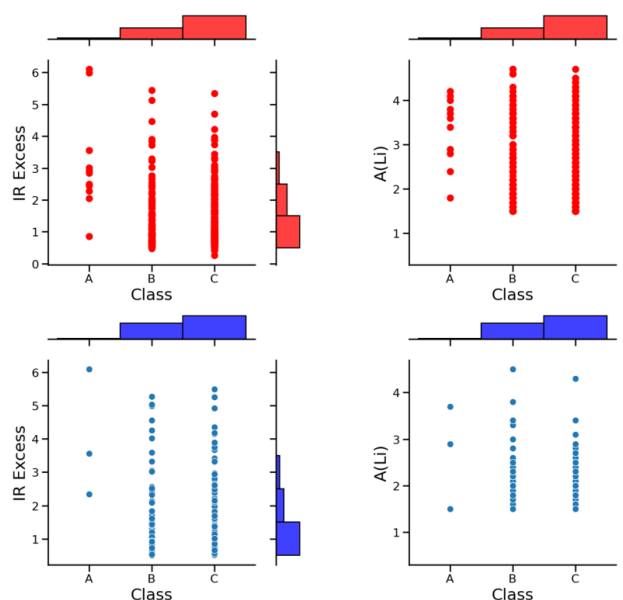


Fig. 1. Distribution of RC and RGB giant stars in different classes of signal-to-noise ratios A, B, and C for the IR excess measured by the difference of WISE bands W1 - W4 in magnitudes related flux densities expressed in Janskys (Jy) (first column) and for the Li abundance in dex (second column). Histograms of these distributions are presented in the right vertical and horizontal scales.

conditions of acceptance or refusal of sources are given in the instruction manual of WISE. After, we will compare the representativeness of the results obtained with the three classes A, B, and C. As a final result, we found 421 RC stars and 196 RGB stars, with a total of 617 stars presenting IR excesses and fulfilling the WISE magnitude colour difference of $W1-W4 \geq 0.5$ considered here as a measure of the presence of an IR excess. The numbers' distribution with the three different classes is 14 stars in class A, 208 in class B, and 395 in class C. A comparison with the work of MA21 for class A using only class A in a sample of 1862 stars gives the following rates: for MA21, it is $3/1862$ or 0.16%, whereas in our case, we have $14/10535$ or 0.13%, which is a quite similar result. For case B, we obtain 1.97%, and for case C, 3.7%. Due to the good distribution representativeness of values of $A(\text{Li})$ and IR excess for classes A, B, and C, as displayed in Fig. 1, we considered in this work that all measurements obtained with classes A, B, and C are reliable to proceed for a general analysis using these parameters. All results of the measurements of the infrared excesses contained in the LAMOST catalogue of Li-rich giant stars are presented in Table 1 for 421 RC giant stars and for 196 RGB giant stars. Table 1 contains all the stellar parameters as presented in the LAMOST catalogue of Li-rich giant stars, to which we added four columns corresponding to the IR excess measurements.

The parameters presented in Table 1 are the name of the object; coordinates; T_{eff} ; $\log g$; $[\text{Fe}/\text{H}]$; $A(\text{Li})$; IR excess; `CC_flag`; `Ph_flag`; class; and the classifications A, B, and C with the respective numbers 1, 2, and 3. We note that our mentioned working catalogue, LAMOST, contains, Li-rich giant stars for the following stellar parameters: T_{eff} between approximately 4000 K and 5500 K, $\log g$ between approximately 1.0 and 3.5, and $[\text{Fe}/\text{H}]$ between approximately -1.7 and 0.4.

Table 1. Stellar parameters of RC and RGB giant stars presenting IR excesses.

OBJECT	Coordinates	T_{eff} (K)	$\log g$	[Fe/H]	A(Li)	IR	CCflag	Phq	Note	Stage
J000108.96+072932.9	00:01:08.96 +07:29:32.9	4731	2.5	-0.2	3.6	1.067	0	AAAC	3	RC
J000151.65+265848.4	00:01:51.65 +26:58:48.4	5071	2.5	-0.5	4.7	1.208	0	AAAC	3	RC
J000851.01+523009.3	00:08:51.01 +52:30:09.3	4797	2.5	-0.1	2.3	1.553	0	AAAC	3	RC
J000920.04+563644.1	00:09:20.04 +56:36:44.1	4830	2.4	-0.3	3.9	1.654	0	AAAC	3	RC
J001154.03+564857.0	00:11:54.03 +56:48:57.0	4785	2.4	-0.2	1.8	0.584	0	AAAC	3	RC
...

Notes. The table includes, in order, the stellar identification, right ascension (RA), declination (DEC), effective temperature (T_{eff}), surface gravity ($\log g$), metallicity ([Fe/H]), lithium abundance (A(Li)), IR excess (IR), the WISE confusion flag, and the WISE photometric flag. The notes indicate the classification of IR sources based on the photometric flag (see text) and evolutionary stage (RC or RGB). This table is shown in part; the complete version is available online as a VizieR catalogue.

2.1. The use of $\log g$ to separate RGB and RC giant stars

Distinguishing between RGB and RC giant stars is not an easy task. The best way to separate them requires the use of asteroseismology. This is due to the fact that RGB and RC stars have different internal structures, and they exhibit different signals of seismic oscillations (Bedding et al. 2011). Normally, without this tool, this distinction is generally made using a standard methodology to obtain the stellar gravities ($\log g$). The main known problem is that if RC giant stars are concentrated around certain specific values of $\log g$, this is not the case for RGB giant stars' $\log g$ values, which occupy a larger range of $\log g$ values, even comprising those corresponding to RC values. Under these conditions, disentangling RC and RGB classes of stars could involve some dubious cases. We proceed to classify the most appropriate general values of $\log g$, guided by results based on those obtained using asteroseismology (Yan et al. 2021, hereafter YA21). YA21 provided a uniquely large sample with a clean determination of evolutionary stages based on asteroseismology. Under these conditions, we adopted the following criteria: for RGB stars, $\log g$ between 2.8 and 3.5; for RC giants, $\log g$ between 2.2 and 2.7. Adopting these conditions, we discarded 88 Li-bright giant stars that have $\log g$ values under 2.2, for which there are no measurements from asteroseismology (following YA21).

The counts of all our RC and RGB giants, all of them presenting IR excesses, as functions of the Li abundance are shown in Fig. 2. YA21 presented a similar distribution, except for Li-rich giant stars, which do not show IR excesses in principle and are based on asteroseismology. To compare both distributions, in Fig. 2 we use short horizontal lines to show the minima and maxima of Figure 1 in YA21. This simple comparison shows that the distributions are similar. We can then conclude that our distribution, based on a $\log g$ discrimination of RGB and RC stars, is similar to that based on asteroseismology. This result indicates that giant stars presenting IR excesses are similar to giant stars not showing IR excesses. The same argument that both classes of objects are similar is presented in the next Sect. 2.2, this time based on metallicities.

The results of our measurements of the infrared excesses based on all the 10535 Li-rich giants in the LAMOST catalogue are shown in Fig. 3. The 421 RC giant stars whose IR excesses have been detected are represented by red points, while the RGB giant stars are represented by blue points. The y-axis contains the Li abundances as measured in the LAMOST catalogue (GA19) from 1.5 up to 4.8. The x-axis contains the measured IR excess values from W1–W4 larger than or equal to 0.5 up to larger magnitudes. In the same figure, we superposed five Li-rich and super-

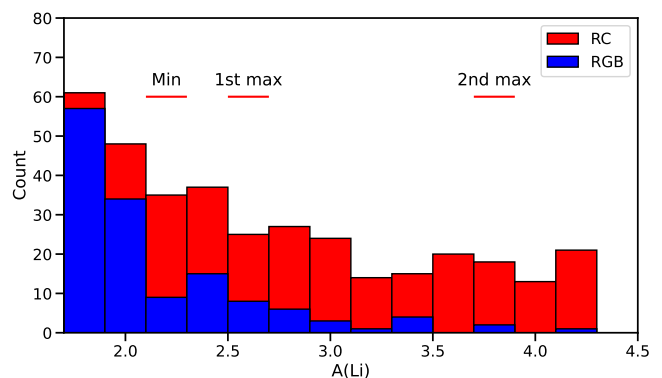


Fig. 2. Counts of giant RC and RGB stars with IR excesses as function of Li abundance in dex as obtained in this work. This figure must be compared with a similar figure of YA21 based on asteroseismology data (Figure 1 in YA21). Using short horizontal lines, we present the regions coincident with the presence of minimums and maximums of the figure of YA21. In our work, we eliminated all bright RC giants stars with $\log g$ values under 2.2 for which no asteroseismology calibration exists following YA21.

Li-rich RG and RC giant stars (green triangles) known in the literature that do not belong to the mentioned catalogue. These stars have the property of producing complex organic and inorganic material in their very strong winds (see Sect. 4.3). These stars are HD 233517, PDS 68, PDS 100, PDS 365, and PDS 485. A simple inspection of Fig. 3 shows that RC giants are dominant among the very Li-rich giant stars. This is not the case for RGB stars, which, apart from a few exceptions of very Li-rich objects, appear concentrated with Li abundance values below ~ 2.6 dex. We must note that several RGB stars with high Li abundances are suspicious due to the mentioned difficulty of separating RGB stars from RC stars. In these conditions, without a seismology criterion, it will be no surprise if some RGB-classified stars with Li abundances over 2.6 dex are misclassified and are, in reality, RC stars.

2.2. Metallicity of li-rich giant stars presenting mass loss

As mentioned before, we found a subgroup of stars containing nearly 6% of the 10,535 studied Li-rich giant stars belonging to the LAMOST catalogue (GA19), presenting evidence of mass loss. One of the main arguments of this work is to affirm that this subgroup is a transitory one, in the sense that the stellar properties of this sub-group are the same as the rest of Li-rich stars,

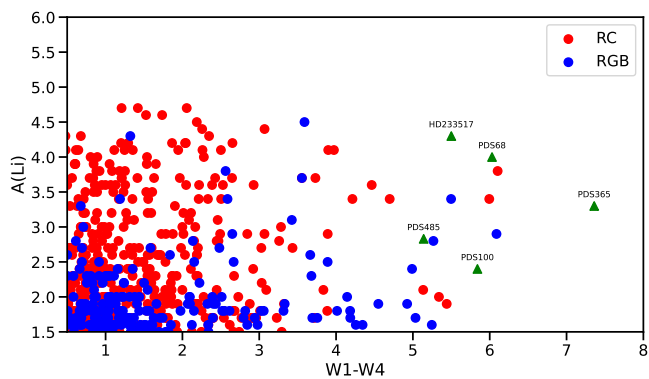


Fig. 3. $A(\text{Li})$ in dex of 421 RC and 196 RGB giant stars obtained in this work in function of IR excesses measured by the difference magnitude WISE colours W1 – W4 larger than or equal to 0.5. RC stars are denoted with red, whereas RGB stars are denoted in blue. Green triangles represent some giant stars not belonging to the LAMOST catalogue (see text).

with the exception that they are transiently ejecting mass. To try to prove this fact, we now use their invariable stellar metallic properties and compare them to the metallicities of Li-rich giant stars not presenting IR excesses, which means not showing indications of the existence of mass loss.

In Fig. 4, we display metallicity histogram distributions of Li-rich giant stars from the LAMOST and GALAH data sets and compare them to our LAMOST Li-rich giants, this time presenting IR excesses. First, we compare those resulting from the same LAMOST data set. In the upper panel of Fig. 4, we show the GA19 distribution without separating RC and RGB giants alongside our distribution containing IR excesses. This results in a similar distribution, which naturally arises because they belong to the same set of data. In the two lower panels, the comparisons are made with the GALAH data set, this time separating RC and RGB giants. The second lower panel, corresponding to RC giants and in which the distributions are normalised, indicates a rather similar behaviour, with both distributions presenting the same Full Width at Half Maximum (FWHM). The third panel corresponds to RGB giants. Here, some differences appear, with the FWHM of GALAH being somewhat larger than our distribution. This difference results from a relatively flat distribution found in GALAH from $-2 < [\text{Fe}/\text{H}] < 0$. This peculiar flat distribution is interpreted by MA21 as eventually being due to multiple signs of Li-enrichment processes at the core of their distribution (see MA21). Regardless of these details concerning the attributed Li enrichments applied only to RGB giants, their distributions of RC giants appear similar to ours.

We conclude that our subgroup of mass-losing giant stars, which includes both RC and RGB stars, has a similar metallic distribution to that of all Li-rich giant stars. In this way, we show that our subgroup is of the same nature as all Li-rich giant stars, with the exception that they are transiently ejecting masses.

3. The general scenario

With this work we present a qualitative general scenario that is valid for a single low-mass giant star to explain the origin of the Li enrichment observed in these stars. The main scenario follows a universal approach in which all low-mass giant stars with masses between $\sim 0.8 M_{\odot}$ and $\sim 2 M_{\odot}$ undergo a short episode of Li enrichment accompanied by the ejection of a circumstellar

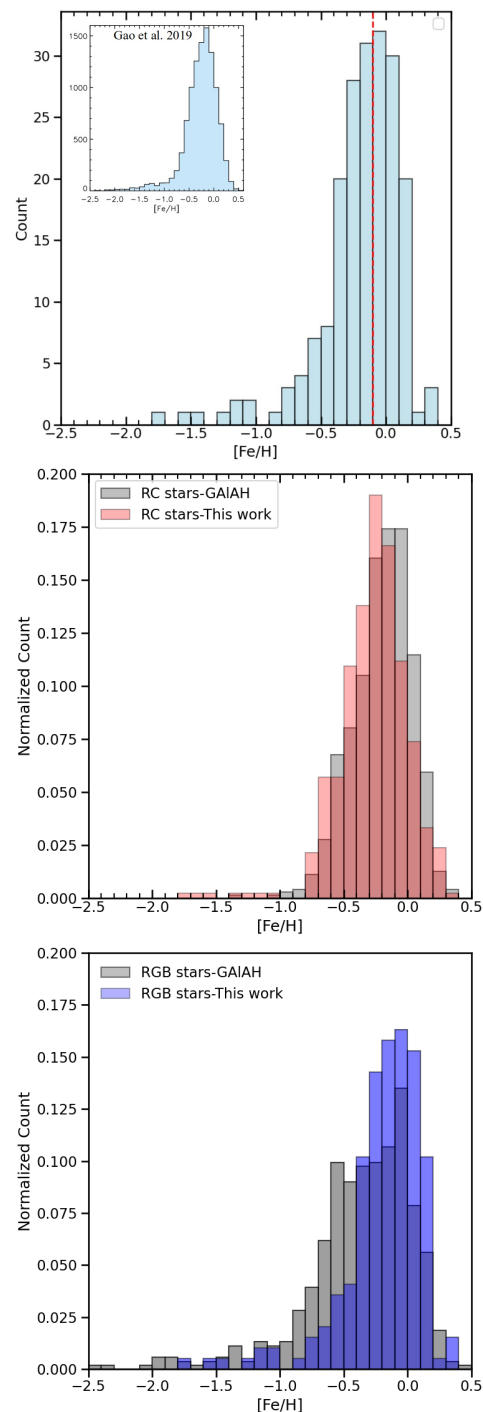


Fig. 4. Comparisons of our distribution of Li-rich giant stars presenting IR excesses as a function of metallicity to the distributions of the same Li-rich giants from the LAMOST and GALAH data sets that do not show these IR excesses.

shell (de la Reza et al. 1996, 1997; de la Reza & Drake 2012). It is considered that the origin of this mass loss resides in the internal angular momentum (AM) evolution of the star. This evolution is provoked by the asteroseismology-observed slow rotation of the stellar core (see a review in Aerts et al. (2019)). How this AM transfer distribution is actually occurred in these stars is not well known. We propose that this distribution consists of a mass transfer between the radiative upper H-burning zone and the external convective envelope (see also de la Reza et al. 2015, hereafter DLR15).

One essential requirement in this scenario is a rapid and sporadic internal transport of the internal mass containing the ${}^7\text{Li}$ as the dominant element; this is from the internal upper H-burning zone before it is destroyed by nuclear proton reactions and up to the external stellar convective layer. This rapid internal upward process is not known, and we speculate that it could be provoked by another sporadic instability, probably of a magnetic nature. Following the nuclear simulations presented by Yan et al. (2018), (hereafter YA18), the required ${}^7\text{Li}$ transport time is only 47 yr for a very Li-rich giant with a Li abundance of 4.5 dex (see Sect. 3.1). Another important part of our scenario consists of this mass transport being sufficiently energetic in order to form low-mass circumstellar shells, which are observed in these Li-rich and very Li-rich giant stars. The evolution of these rapid shells, formation, and ejections (see Sect. 4) represents stellar winds with much larger, episodic stellar mass losses, even with a maximum increase of five orders of magnitude compared to the permanent stellar mass losses of the normal Li-poor giant stars.

The proposed qualitative scenario requires that all stars are suddenly Li enriched, at least one time, during the RGB or RC stages. Are more of these episodes possible? This depends on the repeatability of speculated internal instability and on the reservoir of He^3 available. When this fuel, which originated when the star was on the main sequence, is finished, the Li enrichment stops.

To our knowledge, only two works in the past have used the stellar AM to study the problem of high Li abundance in giant stars: Fekel & Balachandran (1993) and DLR15. However, in the first reference, they considered that a rapidly rotating stellar core was the main trigger mechanism provoking the high Li abundances and producing the IR excesses (see also Fekel et al. 1996). Today, it is known that the stellar core is, on the contrary, slowly rotating. In DLR15, this new condition of the rotating core is taken into account, suggesting internal mass transport as the main avenue to enrich the giant star with fresh Li and provoke the formation of the IR excesses. This represents the general scenario of the present work.

In fact, the detection of slower rotation in the cores of low-mass stellar giant stars using asteroseismology techniques, compared to predictions from standard classical models, has sparked renewed interest in the study of stellar interiors. This core spin-down suggests that there is an efficient redistribution of internal angular momentum transfer at play. However, the specific mechanism for this transfer between the radiative upper H-burning zone and the external convective zone in actual stars has not yet been resolved. Many researchers are currently dedicated to solving this problem, as evidenced by the references provided in recent works (see, e.g. Meduri et al. 2024; Moyano et al. 2023; Dumont 2023; Denissenkov et al. 2024). Both magnetic rotation instability and Tayler instability, driven by differential rotation in giant stars, are competing processes. Meduri et al. (2024) also introduce the important transfer of chemicals from the internal regions to the star's surface, creating another avenue for future developments in this field.

In this context, one partial requirement to try to solve the Li puzzle consists of examining the rapid upward motion of the internal material, where ${}^7\text{Li}$ is the dominant element. This motion considers the travel from the upper H-burning region up to the external convective envelope. Yan et al. (2018), using the conveyor-belt mechanism (Sackmann & Boothroyd 1999), made all the necessary nuclear-reaction simulations in order to result in a very Li-rich giant star with a Li abundance of 4.5 dex. In these simulations (see Figure 3 in YA18), the stellar material containing a standard chemical composition at the stellar convective en-

velope goes down to be processed in the internal radiative zone. There, the original ${}^7\text{Be}$ element increases its abundance up to a maximum due to the constructive nuclear process ${}^3\text{He}({}^4\text{He},\gamma){}^7\text{Be}$. According to YA18, this downward action requires a processing time of 423 yr.

In this internal region with very high temperatures, the ${}^7\text{Li}$ abundance is very low due to the destructive reactions ${}^7\text{Li}(p,\gamma){}^8\text{Be}$ and ${}^7\text{Li}(p,\alpha){}^4\text{He}$. Here, ${}^7\text{Be}$ attains its maximum abundance and begins to increase the ${}^7\text{Li}$ abundance by means of ${}^7\text{Be}(e^-, \gamma){}^7\text{Li}$. Then, the upward conveyor requires a fast motion with a high velocity to bring this material, where ${}^7\text{Li}$ is the dominant element, to the external envelope. This fast motion is necessary to attain cooler regions and avoid the destruction of Li^7 by the mentioned proton processes. YA18 obtains this super Li-rich giant star in an upward time of only 47 yr. During that time, ${}^7\text{Be}$ suffers a moderate abundance decrease (see figure 3 in YA18).

Unfortunately, YA18 does not provide this ${}^7\text{Li}$ velocity, but we can use this time interval of 47 yr to obtain an approximate value for this velocity that can be compared to the necessary upward velocity to transport other elements such as C and N. For these last elements, Eggleton et al. (2008) gave values around 2 cm/s; this is sufficient to mix a stable region with the outer convective envelope in times much shorter than the evolution times given by these authors. By using similar atmospheric scales of this last reference as equal to $10R_{\odot}$, we obtain a velocity of ~ 470 cm/s for this distance with a time of 47 yr for the outward transport of ${}^7\text{Li}$. This last velocity is much larger than that required for C and N. We can conclude that due to this very large difference in velocities, no correlation is expected between the ${}^{12}\text{C}/{}^{13}\text{C}$ ratio and Li. Concerning this correlation, we can refer to the first study that considered field Li-rich giant stars and their corresponding ${}^{12}\text{C}/{}^{13}\text{C}$ ratios, where a complete absence of correlation was found by da Silva et al. (1995). Later, other studies on field giant stars by Aguilera-Gómez et al. (2023) showed that a correlation between these carbon ratios and Fe exists, but no correlation with Li is evident. Additionally, no clear correlations between these two parameters (${}^{12}\text{C}/{}^{13}\text{C}$ and Li) appear to exist among giant stars in very different environments, such as those in open clusters (Gilroy 1989) and among super metal-deficient stars (Molaro et al. 2023).

4. The lithium shell model

Our proposed general scenario for the Li enrichment in low-mass giant stars predicts the ejection of stellar shells characterising quite strong stellar winds, as mentioned before. These shells are the observed IR excesses associated with the Li-rich stars. Initially, these IR sources were discovered and identified using the Infrared Astronomy Satellite (IRAS). Later, Rebull et al. (2015) revisited all these IR sources of Li-rich giant stars by means of the WISE explorer. In the original model (de la Reza et al. 1996, 1997), considering IRAS sources, the shells were immediately detached from the star, ejected, and lost in the interstellar medium. This situation will probably lead to a sort of quasi-explosive situation resembling the Li-flash thermal instability as suggested by Palacios et al. (2006). However, in de la Reza & Drake (2012), a more plausible conceptual physical modification was made without changing the structure of the model. In this new conception, the shells continue to be attached to the star until the completion of the internal Li-enrichment mechanism. Once this enrichment process is finished, the shell detaches from the star and is finally ejected into the interstellar medium. This new detachment concept has the advantage that, contrary to the first model, the size of the shell can be estimated. In any case,

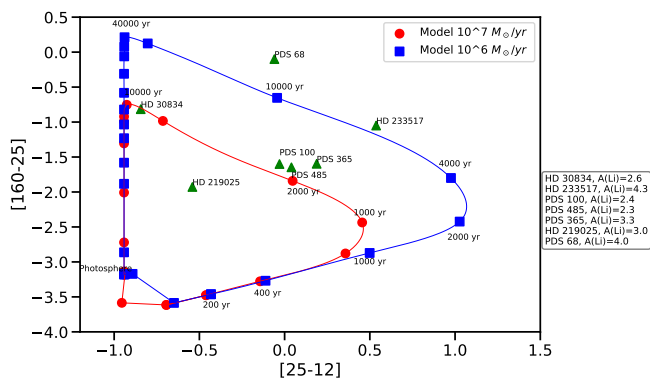


Fig. 5. Model of stellar shell ejections represented here in a colour-colour diagram with wavelengths at $12\mu\text{m}$, $25\mu\text{m}$, and $160\mu\text{m}$, with two loops indicating the growing in time of the shells (see text). The red trajectory is for stellar mass losses of $10^{-7} M_{\odot}/\text{yr}$ and the blue is for $10^{-6} M_{\odot}/\text{yr}$. Green filled triangles indicate observed colours of some giant stars together with their respective Li abundances. Both axes are represented by $[\lambda_1 - \lambda_2] = \log(\lambda_2 F_1) - \log(\lambda_1 F_2)$. The observed fluxes (F) in Jy were obtained from Rebull et al. (2015) and AKARI and HERSCHEL catalogues.

the increase of the shell follows an evolution directly related to a $V_s = R/t$ mode, in which V_s is the velocity of the evolution of the size of the shell and R is the size of the shell. The time t is related to the lifetime of the shell. When the shell detaches from the star, R then measures the size of the shell plus the distance to the star. In a colour-colour diagram (Fig. 5), constructed with IR colours at $12\mu\text{m}$, $25\mu\text{m}$, and $160\mu\text{m}$, we show the evolution paths of the shells. They begin in a box where the giant stars present no IR excesses, which is characterised by normal Li-poor giant stars. As time increases, the shell evolution forms a loop, finally returning to the initial box. Following de la Reza et al. (1996, 1997) and de la Reza & Drake (2012), the sizes of the loops depend mainly on the stellar parameters V_s and stellar mass loss. To a lesser extent, they depend on the stellar radius and the effective temperature.

The model requires low evolution velocities of the shell's expansion, of the order of ~ 2 km/s, to cover the positions of the observed fluxes at those wavelengths. Mean values of the stellar radii of $20 R_{\odot}$ and of the T_{eff} temperatures of 4900 K have been adopted. The shell evolution curves contain the seven Li-rich giant stars with strong IR excesses shown with green triangles in Fig. 5; these are HD 233517, PDS 68, PDS 100, PDS 365, PDS 485, HD 219025, and HD 30834. The Li abundances for each object are mentioned in the same figure. As can be seen in this figure, the stellar episodic mass losses appear dependent on the Li abundances, with very high mass losses of $\sim 10^{-6} M_{\odot}/\text{yr}$ for stars with Li abundances equal to or larger than 4.0 dex. Stars with Li abundances between 2.3 dex and 3.3 dex require slightly lower mass losses of the order of $10^{-7} M_{\odot}/\text{yr}$. It is interesting to note that larger mass losses, meaning more energetic processes, appear necessary to produce larger quantities of Li.

4.1. Considering whether lithium-enriching giant stars are the only ones with IR excesses

In this work, one of the most important points consists of affirming that only giant stars that are in the process of being enriched with new lithium present IR excesses. This means that normal

lithium-poor giants do not show these kinds of IR excesses. The validity of this last strong condition requires a detailed examination of the different surveys to detect IR excesses in giant stars. The majority of the different censuses were completed using the IRAS database, which has been replaced by the much more efficient WISE database. The surveys looking for IR excesses in giant stars were made with very different star samples.

First, Jura (1990), collecting 100 bright G and K giants, noted the absence of IR excesses in G giants and finally selected only two K giants with low fluxes at $60\mu\text{m}$ IRAS. Zuckerman et al. (1995) considered 40,000 giants and found fewer than 300 possible excess giants. For this last survey, we examined their published list of stars and found, among K-type giants, only two objects with significant IRAS excesses. These are HD 19745 and HD 219025, which are known to be very lithium-rich stars (de la Reza & da Silva 1995). Both giants have strong WISE excesses measured by W1 – W4, corresponding to values of 2.3 and 3.7. There is a third known lithium-rich giant with a lithium abundance of ~ 1.9 (HD 30834), measured with lower quality IRAS data, for which a WISE excess cannot be estimated. All the other giant stars on this list have, when WISE measurements are possible, W1–W4 values less than or equal to 0.1, signifying no significant excesses.

Later, Plets et al. (1997) explored a large number of G, K, and M-type giant stars, detecting among the K giants only two Li-rich stars, namely HD 30834 and HD 146850. We searched for all K giants listed in its appendix for which Li abundances are not provided, and we did not find any star with a WISE W1–W4 value larger than 0.1, confirming the absence of real IR-excess giant stars. Later, a census with a similar purpose appeared in Kumar et al. (2015) with a sample of 2000 low-mass K giants. Their results can be divided into two parts. First, they published a list in their Table 1 of 40 lithium-rich giants, which also includes additional giant stars from the literature.

From this list, only seven giants, which are those taken from the literature, have very strong IR excesses with WISE values between 2.3 and 7.3. All of the other lithium-rich stars have WISE values less than or equal to 0.1 and are practically without IR excesses. Secondly, they mention another list containing about two dozen K giants with detectable far-IR excess, and, surprisingly, none of them are lithium-rich giants'. Unfortunately, they do not publish this list, and we have no means to examine it to know which stars they are, their precise number, and what their actual degree of far-IR detectability' is. In an attempt to understand which stars belong to this unknown list, we explored, as far as possible, their three mentioned sources of data. These are Kumar et al. (2011), Liu et al. (2014), and Adamów et al. (2014).

Only the last two references present published lists containing lithium-poor giants. We considered all of the tables (Table 1 for K giants only) in Liu et al. (2014) and Table 1 of Adamów et al. (2014). As a result, we did not find any evidence of lithium-poor normal giants with IR excesses larger than W1–W4 = 0.1.

Kumar et al. (2015), which claimed that the physical coincidences of lithium-rich giants with IR excesses are very rare, are mainly based on a misunderstanding that frequently occurs in the literature, and our work here attempts to dissipate it. This misunderstanding is that lithium-rich giants have a very low probability of having IR excesses because, as seen here, especially in Sect. 4.1, their lithium-rich lifetimes are of the order of 10^7 years, which is much longer than the estimated lifetimes of the lithium short-enrichment episode; this is of the order of 10^4 years, and during this period the giant star presents an IR excess. In conclusion, we can say that, up to this moment, there appear to be no lithium-poor normal giants presenting IR excesses, at

least with our adopted WISE criteria of W1–W4 larger than or equal to 0.5 considered in our work (Table 1) as a real excess. It thus appears that only Li-enriching stars, meaning giant stars in the process of being enriched with fresh Li, are the only ones presenting IR excesses. Future larger volumes of data catalogues of giant stars merging with the WISE database could provide a definitive answer on these matters.

4.2. Lithium stellar lifetimes

The model does not specify the moment when the shell is detached from the star. In any case, the loops close in a few million years when the shell is expected to be completely lost. What is important, however, is that the shells are expected to have short lifetimes. One way to approach a somewhat more realistic lifetime consists of considering an age when the time of the trajectory in the loop coincides with the observed position of the star flux. As seen in Fig. 5, ages are around 2000 yrs for stars with Li abundances between 2.3 and 3.1 dex, and between ~ 5000 yrs and ~ 10000 yrs for stars with larger Li abundances. In this way, we are measuring the time of the fresh Li enrichment in these giant stars. In the same way, we are characterising the lifetimes of this short event. There is another approximate way (not dependent on the preceding model, but more general) to evaluate the lifetimes of Li in giant low-mass stars. This involves simple considerations of the total number of stars studied here. If we take into account the total number of explored giant stars in the LAMOST survey (GA19), which is 814268 stars, the resulting Li-rich giant stars are 10535 with Li abundances equal to or larger than 1.5 dex. This means a fraction of 0.0129. In this work, we detected 421 RC stars and 196 RGB stars representing IR excesses, or a total of 617 stars. This total number represents a fraction of 0.058, or almost 6%, of the Li-rich stars in the LAMOST catalogue. If we consider crude values of the lifetimes of stars in the RGB stage as 10^9 yrs and 10^8 yrs for RC stars, or 1.1×10^9 yrs, we obtain, considering fractions as indicators of lifetimes, that the Galactic Li lifetime is approximately $0.0129 \times 1.1 \times 10^9 = 1.4 \times 10^7$ yrs. Now, the fraction of giant stars with IR excesses or losing mass will be approximately $0.058 \times 1.4 \times 10^7 = 8 \times 10^5$ yr. We note that this value is contained in the total time of the Li enrichment loops of Fig. 5. We saw, however, that in those loops, more realistic lifetimes of the prompt Li enrichment could be one or more orders of magnitude smaller. What we learn here is that if 6% of the stars are being enriched with Li, the remaining 94% of Li-rich stars maintain their new Li for longer periods of $\sim 10^7$ yr. We note, moreover, that this is a general evaluation of the involved future Li-star depletion. In RC giant stars, which represent a different physical situation than RGB stars, much shorter Li depletion times could exist.

4.3. Chromospheric activation and the lithium properties

Using the *Hubble* Space Telescope, we observed the spectra of the four Li-rich giant stars (HD 9746, HD 39853, HD 112127, and HD 787) between $\sim 2460 \text{ \AA}$ and $\sim 2540 \text{ \AA}$ (Drake et al. 2018). The original objective was to measure the two neutral boron lines at 2496.771 \AA and 2497.725 \AA to test the engulfing-planet scenario, as proposed to explain the origin of Li-rich giant stars. To our surprise, we found that the intensity of both the continuum and the spectral UV lines increased apparently according to the growing Li abundances. However, this relation with Li is indirect, via the chromospheric excitation. This is shown in

Fig. 6, where the UV spectra of stars HD 9746, HD 39853, and HD 112127 are presented in order. Their corresponding important stellar parameters, including Li abundance, T_{eff} , and rotational $v \sin i$ velocity, are as follows: for HD 9746: 3.44, 4425 K, and 5.5 km/s; for HD 39853: 2.75, 3900 K, and 1.2 km/s; and for HD 112127: 2.95, 4340 K, and 1.7 km/s. All these parameters are taken from Jorissen et al. (2020), with the exception of the HD 112127 $v \sin i$ value taken from de Medeiros et al. (1996). We note that for HD 9746, de Medeiros et al. (1996) proposed an even larger $v \sin i$ value of 8.7 km/s. It thus appears that the main parameter controlling the intensities of the UV lines is that of the rotational velocity. Jorissen et al. (2020) considered $v \sin i$ values larger than or equal to 5.0 km/s as those of rapid rotators.

The involved emission lines, as shown in Fig. 6, are mainly FeII lines (Judge & Jordan 1991). Among these lines, for example, the 2507 Å and 2509 Å lines are fluorescence lines pumped by H Ly α Johansson & Hamann (1993), pointing to the existence of very strong H Ly α emission. What is important in this picture is that the chromospheres of these stars appear to be activated. For a correlation between activity and high Li abundance, we suggest the works of Fekel & Balachandran (1993) and Drake et al. (2002). Another recent study concerning chromospheric and Li relations, this time involving the He I line at 10830 Å, is that of Sneden et al. (2022). Here, the very Li-rich single giant star HD 233517 (Strassmeier et al. 2015; Fekel et al. 1996), with a Li abundance of 4.3 dex, received special attention. This star has by far the strongest He I 10800 Å and is separated from all the other Li-rich and Li-poor giant stars in the mentioned study. In this aspect, searching for a tighter chromospheric–Li abundance relation, it will be of particular interest to measure the intensity of the He I line at 10830 Å in other very Li-rich and Li-rich giant stars (such as those presented as in Fig. 7 of the next subsection) that have a strong mass loss, such as HD 233517. In the qualitative general scenario presented in this work, the surface rotation of giant stars depends on how the AM transfer is realised. It also depends on the internal rapid upward mass transfer that produces the surface Li enrichment. We can propose that more energetic mass losses will produce more chromospheric activation during their journey from the stellar interiors to the external wind regions. Larger abundances of lithium will then appear to be present mainly in rapid rotators.

Even if the majority of low-mass giant stars appear to be quiet and inactive stars, there is a fraction of them presenting significant UV-emission excess, which shows a good correlation with stellar rotation velocities (Dixon et al. 2020). This rotation-activity relation, which has been largely studied for dwarf stars, applies, according to these authors, to RGB and RC giants.

In this context, and regarding Li-rich giants, it is surprising to see here in Fig. 6 that these few giant stars appear to correlate between UV line intensities and $v \sin i$. Even more surprising is that the measured $v \sin i$ value of the highest intensity UV-emission spectrum star (HD 9746) is 8.7 km/s (de Medeiros et al. 1996) and not 5.5 km/s as shown in the figure.

Regarding Li giants, we propose, as previously mentioned, an extension of the study of chromospheric activity in Li-rich stars by Sneden et al. (2022) using the chromospheric He line at 10830 Å; to this study, we would add rapidly rotating giant stars of varying Li abundances and IR excesses. This can provide more information to examine whether stellar rotation is, in fact, the dominant driver of activity.

Mass-loss rate calculations are also being studied in giant stars by a different approach than the dust-based mass-loss calculations based on IR excesses used here (de la Reza et al. 1996).

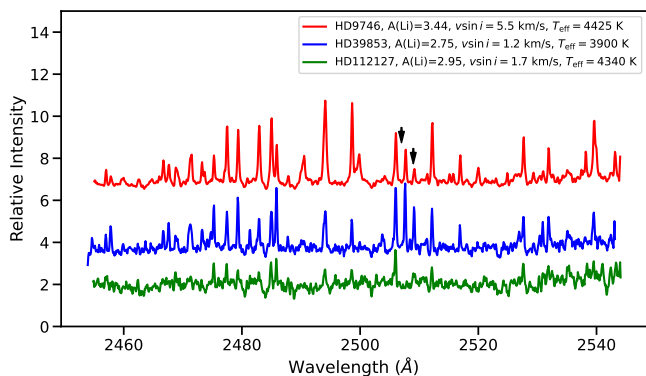


Fig. 6. UV *Hubble* spectra of three Li-rich giant stars –HD 9746, HD 39853, and HD 112127– are shown here (See also Drake et al. 2018) with their respective Li abundances and $v \sin i$ values. Emission lines are mostly due to FeII. The place of the faint neutral boron resonance lines is indicated by arrows.

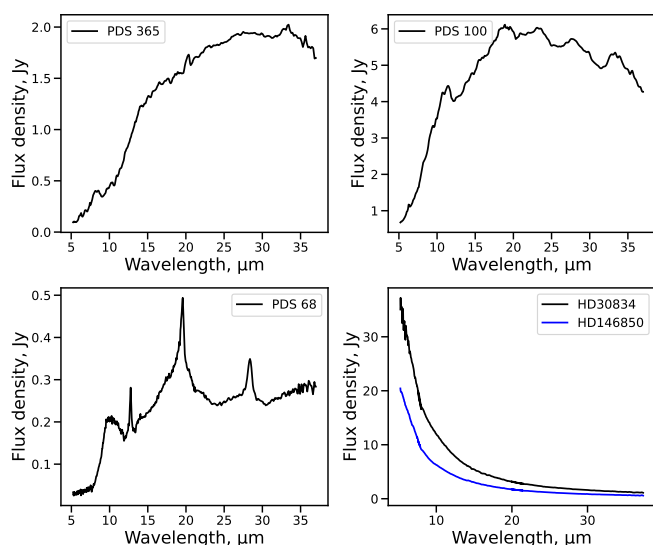


Fig. 7. NIR spectra obtained with Spitzer telescope are shown here for some Li-rich and super Li-rich giant stars: a) PDS 365, $A(\text{Li}) = 3.3$ dex; b) PDS 100, $A(\text{Li}) = 2.4$; c) PDS 68, $A(\text{Li}) = 4.0$; and d) HD 30834, $A(\text{Li}) = 2.6$ and HD 146850, $A(\text{Li}) = 1.6$. The first three stars present a strong emission continuum due to their attached shells, and following our model they are in the sudden Li-enriching stage. In the last two stars, the Li-enrichment process is finished and the shell, which is no longer present, is considered to be ejected, whereas the star keeps its Li for a certain time. Superposed on these emission continuums are localised emission peak features due to the presence of complex aromatic organic and inorganic structures (see DLR15).

These are based on the nonlinear propagation of magnetic-origin Alfvén waves (see among others, Cranmer & Saar 2011; Airapetian et al. 2010). Although discussing these models is beyond the scope of this work, we can mention that they were aimed at reproducing stellar mass-loss values of normal Li-poor giants.

This is the case, for example, of the known K giant star Alpha Tau in Airapetian et al. (2010), with a mass loss of $1.6 \times 10^{-11} M_{\odot}/\text{yr}$. In these conditions, it will be a challenge for these models to reproduce the very brief mass-loss episodes of 10^{-7} – $10^{-6} M_{\odot}/\text{yr}$, as seen in Fig. 5, which are necessary to explain the rapid Li enrichment episodes proposed in our scenario.

4.4. Complex organic and inorganic particles in the winds of very lithium-rich giant stars

The first aromatic organic material (PAH) was detected in the well-known Li-rich giant star HD 233517 (Jura et al. 2006). The observations were realised in the NIR ($5 \mu\text{m} - 38 \mu\text{m}$) spectra by means of the Spitzer telescope. Jura et al. (2006) proposed that this material originated in a hypothetical disc around this star. Later, DLR15 detected complex organic compounds and the presence of inorganic particles in several other Li-rich giant stars. These results indicate that this material is originated in shells around these stars. In DLR15, it was proposed that the observed organic aromatic and aliphatic compounds were formed in the winds by episodic mass losses of the order of $10^{-7} M_{\odot}/\text{yr}$ to $10^{-6} M_{\odot}/\text{yr}$.

Additionally, the inorganic particles resulted from a stellar wind dragging of the debris disc that remained since these were A-type stars on the main sequence. These discs were probably partially or completely eroded by the action of these strong winds. Among the several inorganic particles detected were Forsterite, enstatite, and several other compounds. The main characteristic of the mentioned NIR spectra is the presence of an important continuum emission in which narrow emission features are superposed at very specific wavelengths. The presence of these features enables us to identify the nature of the organic and inorganic material under consideration (see DLR15). As an example, some of these spectra are shown in Fig. 7 corresponding, respectively, to the giant Li-rich stars PDS 365, PDS 100, and PDS 68. These stars are being enriched with Li and are consequently forming a shell represented by strong NRI continuum emission spectra. For illustration and comparison purposes, we show, in the same Fig. 7, two giant stars: HD 30834, a Li-rich star with a Li abundance of ~ 2.6 dex (Takeda & Tajitsu 2017); and a moderately Li-rich star, HD 146850, with a Li abundance of 1.6 dex (Castilho et al. 1999).

Unlike the PDS stars in the figure, these two stars have no shells detected in the NIR between $5 \mu\text{m}$ and $38 \mu\text{m}$ observed by SPITZER; however, HD 30834 has an important observed flux at $160 \mu\text{m}$ (see Fig. 5) suggesting that its shell is detached and presently located at a larger distance from the star. Sadly there are no FIR data for HD 146850. Following our scenario, HD 30834 and HD 146850 have finished their Li-enrichment process but maintain their new Li.

4.5. Lithium properties of red-clump giant stars

Since the first detection of a Li-rich RC star made with the help of asteroseismology by Silva Aguirre et al. (2014), a large contribution to this subject has recently appeared in the literature. We limit ourselves to mentioning these references without writing about them further, except for those relevant to the following discussion concerning our proposed scenario. In chronological order, we mention, among others, the following references: Kirby et al. (2016); Kumar et al. (2020); Schwab (2020); Martell et al. (2021); Mori et al. (2021); Deepak & Lambert (2021); Magrini et al. (2021); Yan et al. (2021); Singh et al. (2021); Zhou et al. (2022); Chanamé et al. (2022); Mallick et al. (2022); Sayeed et al. (2024). A recent work by Susmitha et al. (2024) opens a new avenue to study the effect of metallicity on the Li production in RC giant stars.

In this work, we present new data on 421 RC Li-rich stars with IR excesses. All of these stars cover a wide range of Li abundances, from 1.5 dex up to almost 5 dex, thus presenting important mass-loss properties. Recently, Mallick et al. (2022)

conducted the first study of RC stars considering IR excesses, confirming that the circumstellar shells lost by these stars have short lifetimes of the order of 3000 yr or less, as we mentioned before for all Li-rich giant stars. It must be noted that no work using the He-flashes existing in this evolutionary stage has been able to explain the super Li-rich state of these stars. If our general Li scenario is correct, these stars are being enriched with fresh Li due to their observed IR excesses. We suggest that these same stars may be at least partially forming new Li through He flashes. By adding these two separate Li contributions, we may be able to explain the presence of the observed super-Li-rich RC giant stars.

4.6. Lithium abundance and stellar rotation

There may be a relation between the stellar Li abundance of giant stars and their rotational stellar velocity. This kind of problem is largely mentioned in the literature and is left unanswered. The probable reason for this is the difficult physical mechanisms involved. As an example, we can take the giant stars considered in this work for which we have measurements of the Li abundances and projected rotational velocities. Even though they are not numerous, they can provide a first insight into this question.

These stars have been discussed in various sections of this work and are the following, listed in order of name, Li abundance, and $v \sin i$ in km/s: HD 9746, (3.44, 5.5); HD 30834, (2.6, 2.7); HD 39853, (2.75, 1.2); HD 112127, (2.95, 1.7); HD 219025, (3.0, 23); HD 233517, (4.3, 17.6); PDS 68, (4.0, 5.0); PDS 100, (2.40, 9.5); PDS 365, (3.3, 20); PDS 485, (2.3, 35.0). The references of velocities for the star PDS 100 can be found in Reddy et al. (2002), and for stars PDS 68 and PDS 485 they can be found in Reddy & Lambert (2005). Only three of these stars do not present IR excesses. A simple inspection of these numbers shows that a linear relation between the Li abundance and $v \sin i$ is inexistent, even if all these stars have Li abundances larger than 2.0 dex, and these stars are rapid rotators if we consider rotational velocities larger than 5.0 km/s as rapid rotators, as mentioned in Sect. 4.3. This discussed non-correlation between the Li abundance and $v \sin i$ can be seen in Fig. 8.

Concerning the physical aspects behind this problem, we can first mention, as also presented in Sect. 4.3, that it is mainly the activation of the chromosphere (in our scenario by a mass transfer coming from the stellar interior and crossing the chromosphere) that probably increases the stellar rotation as observed (see Fig. 6). Moreover, this activation is not directly related to the ${}^7\text{Li}$ transport to the external stellar layers.

Another aspect, and maybe the most difficult, is that the rotation of the external stellar envelope of giant stars depends on how the internal transfer of the stellar AM is actually realised, and this is not well known. In conclusion, considering all these problems, it can be natural not to find a one-to-one relation between the Li abundance and rotation. Nevertheless, as mentioned in Sect. 4.3 a general and crude relation exists between rapid stellar rotators and high Li abundances.

5. Discussion and conclusion

Working solely with the LAMOST DR7 LRS catalogue (GA19), which contains 10,535 giant stars with Li abundances ranging from 1.5 dex to 4.9 dex, and the WISE catalogue, we detected 617 Li-rich stars exhibiting IR excesses. To differentiate between RGB and RC giant stars with IR excesses, we employed a classification based on $\log-g$ values. This selection method aligns with

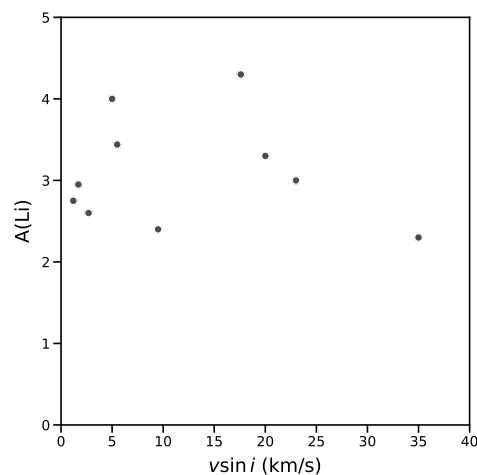


Fig. 8. Projected velocity $v \sin i$ as function of Li abundance for all Li-rich giant stars discussed in this work.

that used by YA21 for Li-rich stars without IR excesses, based on asteroseismology. Our findings demonstrate that the distributions of RGB and RC stars from Yan et al. (2021) and ourselves are comparable.

In this way, we were able to find 421 RC stars and 196 RGB stars with IR excesses, as displayed in Fig. 3, for Li abundances ranging from 1.5 dex up to 4.8 dex. However, their distributions are different. RGB stars have a general maximum Li abundance of around 2.6 dex, whereas RC stars attain maximum values of 4.8 dex. In other words, RC stars are by far the most Li-rich stars.

The distribution of our general qualitative scenario for Li enrichment, which is valid for all single low-mass giant stars, proposes that a sudden Li enrichment occurs, accompanied by an also sudden formation and ejection of circumstellar material. This scenario, described in detail in Sect. 3, includes one speculative key ingredient: the existence of an unknown internal sporadic instability, likely of magnetic origin, that can rapidly transport mass from the upper H-burning zone upwards. This process is part of the unknown evolution of total angular momentum. It is important to note that the key ingredient to form Li-rich and super Li-rich giant stars consists of rapidly transporting the internal material, where ${}^7\text{Li}$ is the dominant element, to the external convective envelope. Based on nuclear simulations found in the literature, we estimate the upward velocity of the ${}^7\text{Li}$ material to be ~ 500 cm/s, a much larger value than that required to transport other elements such as C, which is of the order of 2 cm/s. Due to this significant difference in velocities, an anti-correlation between the ${}^{12}\text{C}/{}^{13}\text{C}$ ratio and Li is expected and is actually observed.

The expected sudden enrichment of Li produces the formation and ejection of circumstellar shells. By applying a shell-model evolution to Li-rich giant stars with large IR excesses from the literature, we find quite short lifetimes for the formation and subsequent ejection of these shells. These lifetimes are on the order of 2000 years and 10000 years, thus characterising the expected rapid Li-enrichment process. The stellar mass-losses involved in this process are very short and several orders of magnitude larger than those of Li-poor giant stars. In this model, the stellar mass losses appear to be proportional to the Li abundances.

Based on the fraction of Li-rich giant stars with respect to Li-poor giant stars in the LAMOST survey, which is 0.0129, and the crude values of the lifetimes of the RGB and RC stages, re-

spectively 10^9 yrs and 10^8 yrs, it is found that the Li Galactic age is approximately 1.4×10^7 yrs. Now, considering our found fraction of stars presenting mass losses, which is 0.058, we infer a total age of Li enrichment of 8×10^5 yrs. This time coincides with the maximum age of the shell ejection for a complete loop in the shell model. We note, however, that more realistic ages of the shells are much shorter: on the order of 10^4 yrs or shorter.

It is expected that the internal mass coming from the stellar interior will traverse the stellar chromospheres and activate them. By means of UV spectra taken with the *Hubble* telescope (Drake et al. 2018) of three Li-rich giant stars, with different Li abundances and different rotational velocities, it is found that their stellar chromospheres appear more activated as they have higher Li abundances. However, this activation relation is more directed relatively to the rotational velocities, with the Li abundances being a consequence of these activations. Chromospheric studies by means of the 10800 He I line by Sneden et al. (2022) show that the very Li-rich giant star HD 233517, which is also a rapid rotator and presents a very strong wind, has by far the strongest observed He I line.

To obtain a tighter chromospheric relation between all these parameters, observing other similar stars such as PDS 68, PDS 100, PDS 365, and PDS 485 with this He I line is recommended. In fact, the majority of these same mentioned stars produce the formation of complex organic and inorganic particles around the stars as observed by the Spitzer Telescope (DLR15). If the organic material is formed in their winds, these winds are sufficiently strong to partially or totally destroy their remaining debris discs when these stars were main-sequence A-type stars, thus producing inorganic material in this way.

The study of the Li properties in RC stars is currently an active field of research. In this work, we present new data on 421 RC Li-rich stars with IR excesses. All of these stars cover a large range of Li abundances, from 1.5 dex up to almost 5 dex, and therefore exhibit significant mass losses. It must be noted that no previous work, utilising the He flashes that occur in this evolutionary stage, has been able to explain the super-Li-rich state of these stars. If our general Li scenario is correct, these stars are currently being enriched with fresh Li due to their observed IR excesses. We suggest that if new Li is produced by means of He flashes in these same stars, at least partially, we can infer that by combining these two separate Li contributions, we may be able to explain the presence of the observed super Li-rich RC giant stars.

Finally, in support of one of the main arguments of our scenario, in which only giant stars that are in the process of being enriched with Li present different degrees of IR excesses or mass loss, we carried out an extensive search of surveys in the literature to determine if normal Li-poor giant stars could present IR excesses. To date, we find no giant stars of this kind showing IR excesses such as those found in Li-enriching giants.

We find that a linear relation between the Li stellar abundances and the rotational velocities is inexistent and discuss the physical reasons for this result in this paper. In conclusion, if our scenario, which is based on a universal fast Li-enrichment-episode process that affects all stars, is correct, this can explain why Li-rich giant stars are so few. This universal approach to the Li problem was first proposed in de la Reza et al. (1996, 1997). Later, other works adopted this point of view, such as Kirby et al. (2012), when the existence of Li-rich giant stars in dwarf galaxies was discovered. Additionally, recent works also adopt this universal approach. As reported by Sayeed et al. (2024), these are from the point of view of observations by Kirby et al. (2016), Kumar et al. (2020), and Mallick et al. (2022), and from expecta-

tations of theoretical models (Schwab 2020; Mori et al. 2021; Magrini et al. 2021). In this respect, we quote the abstract words of Kirby et al. (2012): ‘We consider the possibility that Li enrichment is a universal phase of evolution that affects all stars, and it seems rare only because it is brief’.

6. Data availability

Table 1 is only available at the CDS via anonymous ftp to [cdsarc.u-strasbg.fr](ftp://cdsarc.u-strasbg.fr) (130.79.128.5) or via <http://cdsweb.u-strasbg.fr/cgi-bin/qcat?J/A+A/>.

Acknowledgements. Several people have collaborated with me on various aspects during the elaboration of this work, these are: Hong-Liang Yan, Félix Llorente de Andrés, Carolina Chavero, Natalia A. Drake and Max Snoek. Many thanks to all of them. I also thank the anonymous referee for very useful comments.

References

- Adamów, M., Niedzielski, A., Villaver, E., Wolszczan, A., & Nowak, G. 2014, *A&A*, 569, A55
- Aerts, C., Mathis, S., & Rogers, T. M. 2019, *ARA&A*, 57, 35
- Aguilera-Gómez, C., Chanamé, J., Pinsonneault, M. H., & Carlberg, J. K. 2016, *ApJ*, 829, 127
- Aguilera-Gómez, C., Jones, M. I., & Chanamé, J. 2023, *A&A*, 670, A73
- Aguilera-Gómez, C., Monaco, L., Mucciarelli, A., et al. 2022, *A&A*, 657, A33
- Airapetian, V., Carpenter, K. G., & Ofman, L. 2010, *ApJ*, 723, 1210
- Bedding, T. R., Mosser, B., Huber, D., et al. 2011, *Nature*, 471, 608
- Behrard, A., Sevilla, J., & Fuller, J. 2023, *MNRAS*, 518, 5465
- Cameron, A. G. W. & Fowler, W. A. 1971, *ApJ*, 164, 111
- Carlberg, J. K., Cunha, K., Smith, V. V., & Majewski, S. R. 2012, *ApJ*, 757, 109
- Casey, A. R., Ho, A. Y. Q., Ness, M., et al. 2019, *ApJ*, 880, 125
- Casey, A. R., Ruchti, G., Masseron, T., et al. 2016, *MNRAS*, 461, 3336
- Castilho, B. V., Spite, F., Barbuy, B., et al. 1999, *A&A*, 345, 249
- Castro-Tapia, M., Aguilera-Gómez, C., & Chanamé, J. 2024, *A&A*, 690, A367
- Chanamé, J., Pinsonneault, M. H., Aguilera-Gómez, C., & Zinn, J. C. 2022, *ApJ*, 933, 58
- Charbonnel, C. & Lagarde, N. 2010, *A&A*, 522, A10
- Costa, J. M., da Silva, L., do Nascimento, J. D., J., & De Medeiros, J. R. 2002, *A&A*, 382, 1016
- Cranmer, S. R. & Saar, S. H. 2011, *ApJ*, 741, 54
- da Silva, L., de la Reza, R., & Barbuy, B. 1995, *ApJ*, 448, L41
- de la Reza, R. & da Silva, L. 1995, *ApJ*, 439, 917
- de la Reza, R. & Drake, N. A. 2012, in *Astronomical Society of the Pacific Conference Series*, Vol. 464, *Circumstellar Dynamics at High Resolution*, ed. A. C. Carciofi & T. Rivinius, 51
- de la Reza, R., Drake, N. A., & da Silva, L. 1996, *ApJ*, 456, L115
- de la Reza, R., Drake, N. A., da Silva, L., Torres, C. A. O., & Martin, E. L. 1997, *ApJ*, 482, L77
- de la Reza, R., Drake, N. A., Oliveira, I., & Rengaswamy, S. 2015, *ApJ*, 806, 86
- de Medeiros, J. R., Melo, C. H. F., & Mayor, M. 1996, *A&A*, 309, 465
- Deepak & Lambert, D. L. 2021, *MNRAS*, 505, 642
- Denissenkov, P. A., Blouin, S., Herwig, F., Stott, J., & Woodward, P. R. 2024, *MNRAS*, 535, 1243
- Dixon, D., Tayar, J., & Stassun, K. G. 2020, *AJ*, 160, 12
- Drake, N. A., de la Reza, R., da Silva, L., & Lambert, D. L. 2002, *AJ*, 123, 2703
- Drake, N. A., de la Reza, R., Smith, V. V., & Cunha, K. 2018, in *Astrochemistry VII: Through the Cosmos from Galaxies to Planets*, ed. M. Cunningham, T. Millar, & Y. Aikawa, Vol. 332, 237–241
- Dumont, T. 2023, *A&A*, 677, A119
- Eggleton, P. P., Dearborn, D. S. P., & Lattanzio, J. C. 2008, *ApJ*, 677, 581
- Fekel, F. C. & Balachandran, S. 1993, *ApJ*, 403, 708
- Fekel, F. C., Webb, R. A., White, R. J., & Zuckerman, B. 1996, *ApJ*, 462, L95
- Gao, Q., Shi, J.-R., Yan, H.-L., et al. 2019, *ApJS*, 245, 33
- Gilroy, K. K. 1989, *ApJ*, 347, 835
- Holanda, N., Drake, N. A., & Pereira, C. B. 2020, *AJ*, 159, 9
- Johansson, S. & Hamann, F. W. 1993, *Physica Scripta Volume T*, 47, 157
- Jorissen, A., Van Winckel, H., Siess, L., et al. 2020, *A&A*, 639, A7
- Judge, P. G. & Jordan, C. 1991, *ApJS*, 77, 75
- Jura, M. 1990, *ApJ*, 365, 317
- Jura, M., Bohac, C. J., Sargent, B., et al. 2006, *ApJ*, 637, L45
- Kirby, E. N., Fu, X., Guhathakurta, P., & Deng, L. 2012, *ApJ*, 752, L16
- Kirby, E. N., Guhathakurta, P., Zhang, A. J., et al. 2016, *ApJ*, 819, 135

- Kumar, Y. B., Reddy, B. E., Campbell, S. W., et al. 2020, *Nature Astronomy*, 4, 1059
- Kumar, Y. B., Reddy, B. E., & Lambert, D. L. 2011, *ApJ*, 730, L12
- Kumar, Y. B., Reddy, B. E., Muthumariappan, C., & Zhao, G. 2015, *A&A*, 577, A10
- Li, X.-F., Shi, J.-R., Li, Y., Yan, H.-L., & Zhang, J.-H. 2024, *MNRAS*, 529, 1423
- Liu, Y. J., Tan, K. F., Wang, L., et al. 2014, *ApJ*, 785, 94
- Magrini, L., Lagarde, N., Charbonnel, C., et al. 2021, *A&A*, 651, A84
- Mallick, A., Reddy, B. E., & Muthumariappan, C. 2022, *MNRAS*, 511, 3741
- Martell, S. L., Simpson, J. D., Balasubramaniam, A. G., et al. 2021, *MNRAS*, 505, 5340
- Meduri, D. G., Jouve, L., & Lignières, F. 2024, *A&A*, 683, A12
- Melo, C. H. F., de Laverny, P., Santos, N. C., et al. 2005, *A&A*, 439, 227
- Molaro, P., Aguado, D. S., Caffau, E., et al. 2023, *A&A*, 679, A72
- Mori, K., Kusakabe, M., Balantekin, A. B., Kajino, T., & Famiano, M. A. 2021, *MNRAS*, 503, 2746
- Moyano, F. D., Eggenberger, P., Mosser, B., & Spada, F. 2023, *A&A*, 673, A110
- Palacios, A., Charbonnel, C., Talon, S., & Siess, L. 2006, *A&A*, 453, 261
- Plets, H., Waelkens, C., Oudmaijer, R. D., & Waters, L. B. F. M. 1997, *A&A*, 323, 513
- Rebull, L. M., Carlberg, J. K., Gibbs, J. C., et al. 2015, *AJ*, 150, 123
- Reddy, B. E. & Lambert, D. L. 2005, *AJ*, 129, 2831
- Reddy, B. E., Lambert, D. L., Hrivnak, B. J., & Bakker, E. J. 2002, *AJ*, 123, 1993
- Sackmann, I. J. & Boothroyd, A. I. 1999, *ApJ*, 510, 217
- Sayeed, M., Ness, M. K., Montet, B. T., et al. 2024, *ApJ*, 964, 42
- Schwab, J. 2020, *ApJ*, 901, L18
- Siess, L. & Livio, M. 1999, *MNRAS*, 308, 1133
- Silva Aguirre, V., Ruchti, G. R., Hekker, S., et al. 2014, *ApJ*, 784, L16
- Singh, R., Reddy, B. E., Campbell, S. W., Kumar, Y. B., & Vrand, M. 2021, *ApJ*, 913, L4
- Smiljanic, R., Franciosini, E., Bragaglia, A., et al. 2018, *A&A*, 617, A4
- Snedden, C., Afşar, M., Bozkurt, Z., et al. 2022, *ApJ*, 940, 12
- Soares-Furtado, M., Cantiello, M., MacLeod, M., & Ness, M. K. 2021, *AJ*, 162, 273
- Stephan, A. P., Naoz, S., Gaudi, B. S., & Salas, J. M. 2020, *ApJ*, 889, 45
- Strassmeier, K. G., Carroll, T. A., Weber, M., & Granzer, T. 2015, *A&A*, 574, A31
- Susmitha, A., Mallick, A., & Reddy, B. E. 2024, *ApJ*, 966, 109
- Takeda, Y. & Tajitsu, A. 2017, *PASJ*, 69, 74
- Tayar, J., Carlberg, J. K., Aguilera-Gómez, C., & Sayeed, M. 2023, *AJ*, 166, 60
- Wallerstein, G. & Sneden, C. 1982, *ApJ*, 255, 577
- Yan, H.-l. & Shi, J.-r. 2022, *Chinese Astron. Astrophys.*, 46, 1
- Yan, H.-L., Shi, J.-R., Zhou, Y.-T., et al. 2018, *Nature Astronomy*, 2, 790
- Yan, H.-L., Zhou, Y.-T., Zhang, X., et al. 2021, *Nature Astronomy*, 5, 86
- Zhang, X., Jeffery, C. S., Li, Y., & Bi, S. 2020, *ApJ*, 889, 33
- Zhou, Y., Wang, C., Yan, H., et al. 2022, *ApJ*, 931, 136
- Zuckerman, B., Kim, S. S., & Liu, T. 1995, *ApJ*, 446, L79